ORIGINAL RESEARCH ARTICLE

Human myocardial mitochondrial oxidative capacity is impaired in mild acute heart transplant rejection

Daniel Scheiber[1,2,3], Elric Zweck[1,2,3], Sophie Albermann[1,2,3], Tomas Jelenik[2,3], Maximilian Spieker[1], Florian Bönner[1], Patrick Horn[1], Heinz-Peter Schultheiss[4], Ganna Aleshcheva[4], Felicitas Escher[4], Udo Boeken[5], Payam Akhyari[5], Michael Roden[2,3,6,7], Malte Kelm[1,6], Julia Szendroedi[2,3,6,7,8,9] and Ralf Westenfeld[1]*

[1]*Division of Cardiology, Pulmonology and Vascular Medicine, Medical Faculty, Heinrich-Heine University, Moorenstraße 5, Düsseldorf, 40225, Germany;* [2]*Institute for Clinical Diabetology, German Diabetes Center, Leibniz Center for Diabetes Research, Heinrich Heine University, Düsseldorf, Germany;* [3]*German Center for Diabetes Research (DZD e. V.), Partner Düsseldorf, München-Neuherberg, Germany;* [4]*Institute for Cardiac Diagnostics and Therapy (IKDT), Berlin, Germany;* [5]*Department of Cardiac Surgery, Heinrich-Heine University, Düsseldorf, Germany;* [6]*Cardiovascular Research Institute Düsseldorf, Medical Faculty, Heinrich-Heine University, Düsseldorf, Germany;* [7]*Division of Endocrinology and Diabetology, Medical Faculty, Heinrich-Heine University, Düsseldorf, Germany;* [8]*Department of Internal Medicine I and Clinical Chemistry, University Hospital Heidelberg, Heidelberg, Germany; and* [9]*Institute for Diabetes and Cancer (IDC) & Joint Heidelberg-IDC Translational Diabetes Program, Helmholtz Center Munich, Neuherberg, Germany*

Abstract

Aims   Acute cellular rejection (ACR) following heart transplantation (HTX) is associated with long-term graft loss and increased mortality. Disturbed mitochondrial bioenergetics have been identified as pathophysiological drivers in heart failure, but their role in ACR remains unclear. We aimed to prove functional disturbances of myocardial bioenergetics in human heart transplant recipients with mild ACR by assessing myocardial mitochondrial respiration using high-resolution respirometry, digital image analysis of myocardial inflammatory cell infiltration, and clinical assessment of HTX patients. We hypothesized that (i) mild ACR is associated with impaired myocardial mitochondrial respiration and (ii) myocardial inflammation, systemic oxidative stress, and myocardial oedema relate to impaired mitochondrial respiration and myocardial dysfunction.

Methods and results   We classified 35 HTX recipients undergoing endomyocardial biopsy according International Society for Heart and Lung Transplantation criteria to have no (0R) or mild (1R) ACR. Additionally, we quantified immune cell infiltration by immunohistochemistry and digital image analysis. We analysed mitochondrial substrate utilization in myocardial fibres by high-resolution respirometry and performed cardiovascular magnetic resonance (CMR). ACR (1R) was diagnosed in 12 patients (34%), while the remaining 23 patients revealed no signs of ACR (0R). Underlying cardiomyopathies (dilated cardiomyopathy 50% vs. 65%; $P = 0.77$), comorbidities (type 2 diabetes mellitus: 50% vs. 35%, $P = 0.57$; chronic kidney disease stage 5: 8% vs. 9%, $P > 0.99$; arterial hypertension: 59% vs. 30%, $P = 0.35$), medications (tacrolimus: 100% vs. 91%, $P = 0.54$; mycophenolate mofetil: 92% vs. 91%, $P > 0.99$; prednisolone: 92% vs. 96%, $P > 0.99$) and time post-transplantation (21.5 ± 26.0 months vs. 29.4 ± 26.4 months, $P = 0.40$) were similar between groups. Mitochondrial respiration was reduced by 40% in ACR (1R) compared with ACR (0R) (77.8 ± 23.0 vs. 128.0 ± 33.0; $P < 0.0001$). Quantitative assessment of myocardial CD3^{+}-lymphocyte infiltration identified ACR (1R) with a cut-off of >14 CD3^{+}-lymphocytes/mm^{2} (100% sensitivity, 82% specificity; $P < 0.0001$). Myocardial CD3^{+} infiltration ($r = -0.41$, $P < 0.05$), systemic oxidative stress (thiobarbituric acid reactive substances; $r = -0.42$, $P < 0.01$) and myocardial oedema depicted by global CMR derived T2 time ($r = -0.62$, $P < 0.01$) correlated with lower oxidative capacity and overt cardiac dysfunction (global longitudinal strain; $r = -0.63$, $P < 0.01$).

Conclusions   Mild ACR with inflammatory cell infiltration associates with impaired mitochondrial bioenergetics in cardiomyocytes. Our findings may help to identify novel checkpoints in cardiac immune metabolism as potential therapeutic targets in post-transplant care.

Introduction

Heart transplantation (HTX) remains the gold standard for the treatment of refractory end-stage heart failure (HF).[1] Advances in immunosuppressive therapy, careful donor and recipient selection, as well as prevention and treatment of opportunistic infections have improved long-term survival of transplant recipients.[2] Acute cellular rejection (ACR) is diagnosed in approximately 10–15% of all heart transplant recipients, particularly within the first 2 years following transplantation.[2–4] Quantity and degree of ACR episodes are related to onset of cardiac allograft vasculopathy and increased mortality.[5]

Acute cellular rejection is diagnosed by light microscopy of endomyocardial tissue specimens with predominantly lymphocytic mononuclear inflammation. Significant grades of rejection show evidence of cardiac myocyte injury or necrosis.[4] Immunohistochemistry revealed that T lymphocytes are the predominant mononuclear cells in ACR.[6]

Acute cellular rejection is graded according to the International Society for Heart and Lung Transplantation (ISHLT) nomenclature.[4] The grading system separates no rejection (0R) from mild (1R), moderate (2R), and severe rejection (3R).[4] Although most heart transplant recipients with mild ACR are asymptomatic[5] and do not require treatment in the vast majority of cases, there is evidence for prognostic relevance of diffuse mild (IB, 1990 ISHLT ACR classification) ACR.[7] Brunner-La Rocca *et al*. observed a progress of about 20% of untreated Grade 1R ACR to higher rejection grades without a change of treatment.[8]

Myocardial energy consumption exceeds that of any other organ. About 90% of myocardial energy production is derived from mitochondrial oxidative phosphorylation (OXPHOS), fuelled by beta-oxidation of fatty acids, pyruvate oxygenation, and the tricarboxylic acid cycle.[9,10] Against this background, it does not surprise that disturbed mitochondrial bioenergetics have been assigned a central role in HF pathophysiology.[11–13] Growing evidence also indicates a functional role of mitochondria in arrhythmogenesis.[14] Stride *et al*. observed impaired OXPHOS capacity in myocardial tissue specimens of patients with left ventricular (LV) systolic dysfunction undergoing LV assist device implantation compared with control patients with a preserved LV ejection fraction undergoing cardiac valve surgery.[15] Recently, we established high-resolution respirometry (HRR) in transcatheter endomyocardial biopsies (EMB) in comparison with tissue specimens harvested during heart surgery, enabling reliable metabolic characterization of myocardial mitochondrial function in humans not undergoing heart surgery.[16]

Studies on myocardial mitochondrial respiration after HTX in humans are very limited. While murine data suggest disturbances in mitochondrial oxidative pathways in ACR,[17,18] only one study in HTX patients has indicated disturbances in myocardial mitochondrial respiration.[19] Just recently, Romero *et al*. described a decreased activity of mitochondrial-related genes in ACR, suggesting a rejection-associated mitochondrial impairment.[20] We thought to extend these findings, by providing a comprehensive functional, clinical, and immunohistochemical characterization of HTX recipients and cardiac tissue specimens.

We aimed to prove functional disturbances of myocardial bioenergetics in human heart transplant recipients with mild ACR by assessing myocardial mitochondrial respiration using HRR, digital image analysis of myocardial inflammatory cell infiltration, and clinical assessment of HTX patients. We hypothesized that mild ACR is characterized by impaired myocardial mitochondrial respiration and relates to cellular inflammation, oxidative stress as well as myocardial oedema and impaired LV function.

Methods

Study protocol

The trial was approved by the institutional review board at Heinrich-Heine-University Duesseldorf (Study Number: 5263R; subanalysis of the ClinicalTrials.gov registration number NCT03386864). All procedures conformed to World's Medical Association Declaration of Helsinki and the ISHLT Ethics statement. Before inclusion, all participants gave written informed consent.

Patient recruitment

Between 09/2016 and 06/2017, we enrolled 35 adult (>18 years) heart transplant recipients, undergoing routine transcatheter EMB at the University Hospital of the Heinrich-Heine-University Düsseldorf (*Table 1*) in this cross-sectional, single-centre trial (*Table 1*).

Endomyocardial biopsy

Four to five tissue specimens from the interventricular septum were acquired under standard fluoroscopic-guided conditions for histochemistry. Two additional biopsies weighing approximately 1 mg were placed in mitochondrial preservation medium for HRR.[16] Cardiac index as measure of cardiovascular function was assessed during right heart catheterization.[16]

Histology

Endomyocardial tissue specimens were analysed by cardiac transplant pathologists according to ISHLT criteria.[4] Diagnosis

Table 1 Patient characteristics

	All patients (n = 35)	ACR (0R) (n = 23)	ACR (1R) (n = 12)	P value
Anthropometry				
Sex (% male)	83	83	83	>0.99
Age (years)	55 ± 12	57 ± 13	53 ± 10	0.32
BMI (kg/m^2)	25.9 ± 4.4	26.2 ± 4.3	25.3 ± 4.7	0.44
Previous ICM (%)	46	39	58	0.55
Previous DCM (%)	60	65	50	0.77
Comorbidities				
T2DM (%)	40	35	50	0.57
CKD Stage 5 (%)	9	9	8	>0.99
Arterial hypertension (%)	40	30	59	0.35
Cardiac characteristics				
Heart rate (bpm)	80 ± 15	79 ± 16	81 ± 12	0.79
LV ejection fraction (%)	67 ± 7	69 ± 7	64 ± 3	0.12
Cardiac index (L/min/m^2)	2.9 ± 0.9	2.9 ± 1.0	2.7 ± 0.6	0.92
Functional class (%)				0.42
NYHA I	46	48	42	
NYHA II	40	48	33	
NYHA III	14	943	25	
Time post HTX (months)	26.7 ± 26.2	29.4 ± 26.4	21.5 ± 26.0	0.40
Donor's age (years)	42.7 ± 13.0	43.4 ± 13.7	41.3 ± 12.1	0.65
Donor's sex (% male)	60	69	42	0.55
Donor's BMI (kg/m^2)	25.7 ± 3.3	25.9 ± 4.0	25.4 ± 1.6	0.71
Clinical chemistry				
HsTropT (ng/L)	39 ± 34	30 ± 25	58 ± 45	0.12
NT-proBNP (pg/mL)	1806 ± 2816	846 ± 802	3551 ± 4168	0.07
Creatinine (mg/dL)	1.4 ± 0.6	1.3 ± 0.4	1.5 ± 0.8	0.41
Cystatin C (mL/L)	1.7 ± 0.8	1.6 ± 0.6	2.0 ± 0.9	0.38
CRP (mg/dL)	0.71 ± 1.35	0.67 ± 1.6	0.75 ± 0.76	0.05*
Haemoglobin (g/dL)	12.4 ± 1.7	12.4 ± 1.9	12.3 ± 1.4	0.91
LDL cholesterol (mg/dL)	106 ± 38	102 ± 27	113 ± 54	0.45
HbA1c (%)	6.3 ± 1.9	6.1 ± 1.0	6.8 ± 3.0	0.80
HbA1c (mmol/mol)	45.6 ± 20.9	43.1 ± 10.4	50.3 ± 32.5	0.87
Medication				
Tacrolimus (%)	94	91	100	0.54
MMF (%)	91	91	92	>0.99
Everolimus (%)	14	17	8	0.64
Prednisolone (%)	94	96	92	>0.99
Loop diuretics (%)	63	52	83	0.14
ACE inhibitor (%)	29	30	25	>0.99
Calcium channel inhibitor (%)	43	39	50	0.72
Beta receptor blocker (%)	31	30	33	>0.99
Statin (%)	91	91	92	>0.99
Acetyl salicylate (%)	86	83	92	0.64
Insulin (%)	20	13	33	0.19
Metformin (%)	6	8	0	0.54

ACE, angiotensin converting enzyme; AU, arbitrary unit; BMI, body mass index; CKD, chronic kidney disease; CRP, c-reactive protein; HbA1c, haemoglobin A1c; HsTropT, high-sensitivity troponin T; HTX, heart transplantation; DCM, dilated cardiomyopathy; ICM, ischemic cardiomyopathy; LDL, Low-density lipoprotein; LV, left ventricle; MMF, mycophenolate mofetil; NT-proBNP, N-terminal-pro brain natri-uretic peptide; T2DM, type 2 diabetes mellitus.
Means ± SD; P values calculated with unpaired t-test/Mann–Whitney test, Fisher's exact test, χ^2 test.

of ACR was established using light microscopy before CD3 immunohistochemistry. Pathologists were blinded to mitochondrial respiration data and cardiovascular magnetic resonance (CMR) results.

Immunohistochemistry

We performed immunohistochemistry for characterization and digital image analysis of inflammatory infiltrates.[21] CD3$^+$ lymphocytes were stained with CD3 antibody (Dako; dilution 1:25). Additionally, myocardial inflammation was diagnosed by CD11a+/lymphocyte function-associated antigen (LFA)-1 + lymphocytes/mm^2 (Immuno Tools, Friesoythe, Germany), CD11b+/Mac-1 + macrophages/mm^2 (ImmunoTools, Friesoythe, Germany), CD45R0 + T memory cells (Dako, Glostrup, Denmark), and perforin+ cytotoxic cells/mm^2 (BD Bioscience, San Jose, California). EnVision peroxidase-conjugated anti-mouse antibody (DakoCytomation) was used as a secondary enhancing antibody. Immunohistological staining was visualized using 3-amino-9-ethylcarbazole (Merck, Darmstadt, Germany) as chromogenic substrate. Slides were counterstained in haematoxylin and mounted with Kaiser's gelatine R (Merck). Immunoreactivity was

quantified by digital image analysis at 200 times magnification. Calculated objects were related to square millimetre (mm^2).

Myocardial bioenergetics

We performed HRR in saponine-permeabilized right ventricular EMB immediately after tissue harvesting using the Oxygraph-2k (OROBOROS Instruments, Innsbruck, Austria) as previously reported.[22] Investigators were unaware of the histologic rejection diagnosis at the time of respiration analysis. Briefly, substrates were applied in the following order (in mM): 2 malate, 1 octanoyl-carnitine, 2.5 ADP for the electron transferring flavoprotein complex (CETF), 10 glutamate for electron transport chain (ETC) complex I respiration, 10 succinate for ETC complex II respiration, 0.01 cytochrome C, 0.005 oligomycin, stepwise titration of 0.2 μM carbonyl cyanide-trifluoromethoxyphenylhydrazone (FCCP) for uncoupled respiration and 5 μM antimycin A. Oxidative capacity was quantified as tissue weight-normalized oxygen consumption at saturating levels of oxygen, ADP and substrates (State 3 respiration). Respiratory control ratio and leak control ratio were calculated as state 3 divided by respiration after addition of oligomycin (state 4o) and state 4o divided by uncoupled respiration (state u), respectively.[22]

Markers of systemic oxidative stress

Serum samples were stored at −80°C and thawed for 1 h on ice prior to measurements.[23] Thiobarbituric acid reactive substances, reflecting lipid peroxidation, were measured fluorometrically (BioTek Instruments, Inc., Winooski, USA) at an excitation wavelength of 544 nm and emission wavelength of 590 nm. Static redox potential (static ORP) and antioxidant capacity were measured using the RedoxSys® (Aytu Bioscience, Englewood, USA).

Cardiovascular magnetic resonance

In participants not presenting with contraindications (e.g. metal implants, defibrillators, or limiting obesity), CMR was conducted on the same day or 1 day after harvesting of the EMB (*n* = 21/35) using a 1.5 T scanner (Achieva, Philips, Best, The Netherlands) with a 32 channel phased array coil. In addition to standard protocols for measuring ventricular volumes and function, LV T2 relaxation time was quantified using the Gradient and SpinEcho (GraSE) sequence as described previously.[24]

Cardiovascular magnetic resonance feature tracking was performed to measure global LV longitudinal strain using a semiautomatic contour tracing software (LV Analysis, TomTec, Unterschleissheim, Germany).

Statistics

Statistical analyses were conducted with GraphPad Prism 7.0 (GraphPad Software, Inc., La Jolla, USA). Normality for continuous variables was tested using the Shapiro–Wilk test. Normally distributed data were presented as means ± standard deviation. Groups were compared using unpaired two-tailed *t*-test when normally distributed or using Mann–Whitney test for non-parametric data. Contingency tables were analysed using Fischer's exact test and χ^2 test if more than two categories were analysed. Correlations in figures of normally distributed data are portrayed with univariate linear regression lines and assessed using Pearson correlation, whereas non-parametric data are described using Spearman's rank correlation. Receiver operator characteristic (ROC) analysis was performed to generate threshold values with respect to optimal sensitivities, specificities, and areas under the curve. Statistical significance threshold was $P < 0.05$.

Results

Patients' characteristics

Out of 35 enrolled heart transplant recipients, 12 had ACR (1R) while 23 had no evidence of ACR (0R) (*Table 1*). There was no case of acute humoral rejection. There were no adverse events associated to EMB. Distribution of sex, age, body mass index, pre-existing cardiomyopathies and medium time post-HTX to study enrolment was comparable between ACR (1R) and ACR (0R) patients (*Table 1*). More than 90% of the enrolled patients received immunosuppressive triple therapy consisting of tacrolimus, mycophenolate mofetil (MMF) and prednisolone (*Table 1*). High sensitive troponin T and NT-proBNP values tended to be elevated in ACR (1R) (*Table 1*).

Myocardial oxidative capacity is impaired in ACR (1R)

In ACR (1R), myocardial mitochondrial oxidative capacity in state III respiration on beta-oxidation related respiration on the fatty acid octanoyl-L-carnitine for CETF was 37% lower than in ACR (0R). Likewise, state III respiration on a mixed protocol of fatty acids and glutamate for ETC complex I respiration was 39% lower in ACR (1R) [77.8 ± 23.0 vs. 128.0 ± 33.0 ($pmol*s^{-1}*mg^{-1}$); $P < 0.0001$; *Figure 1*]. Similarly, ETC complex II respiration following addition of succinate was reduced by 40% in ACR (1R) compared with ACR (0R) [114.1 ± 42.1 vs. 188.8 ± 57.3 ($pmol*s^{-1}*mg^{-1}$); $P < 0.001$; *Figure 1*].

After stepwise titration of FCCP, uncoupled respiration remained persistently 30% lower in ACR (1R) compared with ACR (0R) (*Figure 1*). Respiratory control ratio was also lower

Figure 1 Lower ventricular myocardial mitochondrial oxidative capacity in mild heart transplant rejection. (A, B, C, D) Myocardial mitochondrial respiration with different substrates is lower in mild ACR (1R) compared with no ACR (0R). Substrates used were octanoyl-L-carnitine (for CETF), glutamate (for CI), succinate (for CII), and carbonyl cyanide-trifluoromethoxyphenylhydrazone (FCCP) for uncoupled respiration. (E) Coupling efficiency with respiratory control ratio (RCR) as state 3 divided by state 4o. (F) Intrinsic uncoupling of the respiratory chain, determined with leak control ratio (LCR) as state 4o divided by uncoupled respiration. Data are means ± SEM. *$P < 0.05$, **$P < 0.01$, ***$P < 0.001$, ****$P < 0.0001$ (unpaired t-tests in all figures); $n = 23$ ACR (0R) vs. 12 ACR (1R). AU, arbitrary unit; CETF, electron transferring flavoprotein complex; CI, respiratory chain complex I; CII, respiratory chain complex II.
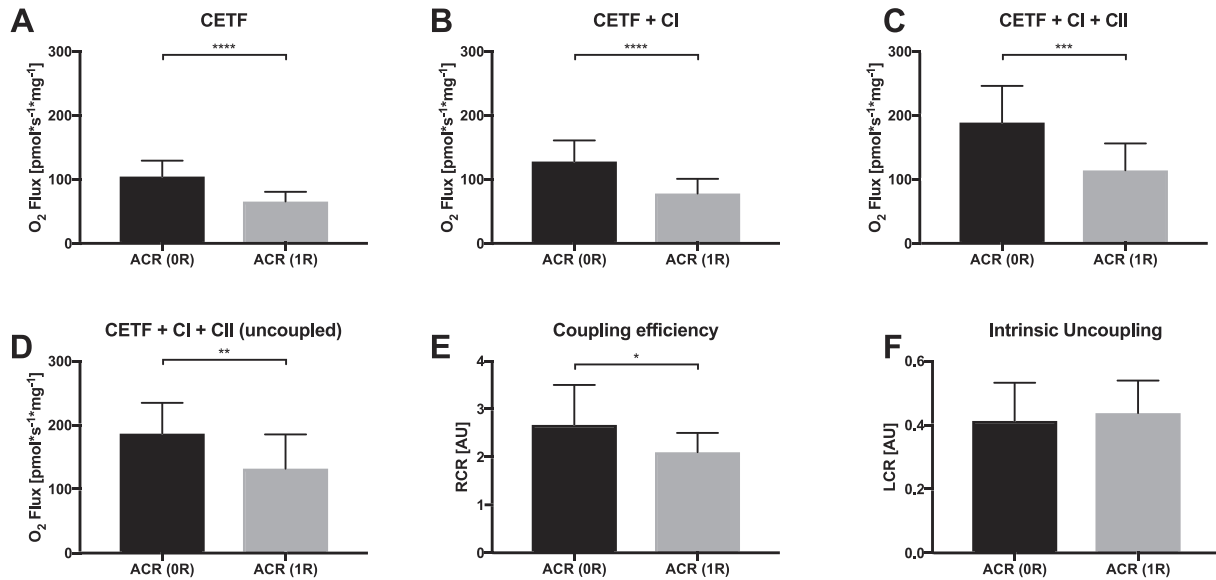
in ACR (1R) [2.7 ± 0.8 vs. 2.1 ± 0.4 (AU), $P = 0.03$], indicating less effective ATP synthesis (*Figure 1*).

ACR (1R) features myocardial inflammatory cell infiltration

Immunohistochemistry revealed myocardial infiltration with inflammatory cells in ACR (0R) (8.8 ± 11.2 cells/mm^2) (*Figure 2*; *Table 2*). Digital image analysis for quantitative assessment of inflammatory cell infiltration discriminated between ACR (1R) and ACR (0R) revealing about four times higher infiltration of CD3$^+$ T lymphocytes in ACR (1R) [39.3 ± 17.9 vs. 8.8 ± 11.2 (cells/mm^2); $P < 0.0001$] and a five times higher expression of LFA in ACR (1R) compared with ACR (0R) [88.2 ± 60.5 vs. 16.4 ± 11.9 (cells/mm^2); $P < 0.0001$] (*Table 2*). Correlating time post-transplantation to inflammatory cell infiltration, there was no significant association (CD3$^+$: $r = -0.14$, $P = 0.44$; LFA-1: $r = -0.04$, $P = 0.83$). ROC analysis for infiltrating CD3$^+$ T lymphocytes in myocardial tissue specimens with a cut-off value of 14 CD3$^+$ cells/mm^2 distinguished ACR (0R) vs. ACR (1R) with a sensitivity of 100% and a specificity of 82% ($P < 0.0001$; *Figure 3*).

Other important markers of myocardial inflammation like perforin, a glycoprotein responsible for pore formation in cell membranes of target cells, macrophage-1 antigen (Mac-1), mediating endothelial cell adhesion and CD45R0, a member of leucocyte common antigen family, expressed largely on previously activated or memory T cells were increased in ACR (1R) (*Table 2*).[25–27]

Figure 2 Immunohistochemical staining of CD3$^+$ lymphocytes in endomyocardial biopsies of patients with and without mild cellular heart transplant rejection. Representative sections of immunohistochemical staining of CD3$^+$ lymphocytes in representative endomyocardial biopsies of patients without ACR (0R) (A) and with mild cellular heart transplant rejection ACR (1R) (B). 200× magnification.

Table 2 Computer-based quantitative assessment of immunohistochemical staining of infiltrate phenotype and cell adhesion molecule expression

	ACR (0R) (n = 22)	ACR (1R) (n = 12)	P value
Cells/mm^2			
CD3	8.8 ± 11.2	39.3 ± 17.9	<**0.0001******
LFA-1	16.4 ± 11.9	88.2 ± 60.5	<**0.0001******
Perforin	0.39 ± 1.1	12.0 ± 37.8	0.058
MAC-1	32.9 ± 23.7	68.1 ± 45.1	**0.019***
CD45R0	41.5 ± 20.0	94.4 ± 57.1	**0.0004*****

CD, cluster of differentiation; LFA, lymphocyte function-associated antigen; MAC, macrophage.
Means ± SD; *P* values calculated with unpaired *t*-test/Mann–Whitney test.

Figure 3 Receiver operating characteristic (ROC) for CD 3$^+$ cells (mm^2). ROC for CD 3$^+$ cells/mm^2 in heart transplant recipients with no ACR (0R) vs. mild ACR (1R) heart transplant rejection); *n* = 19 ACR (0R) vs. 12 ACR (1R).

>14 CD 3$^+$ cells [mm^2]

Sensitivity: 100%
Specifity: 82%
P <0.0001
AUC 0.94
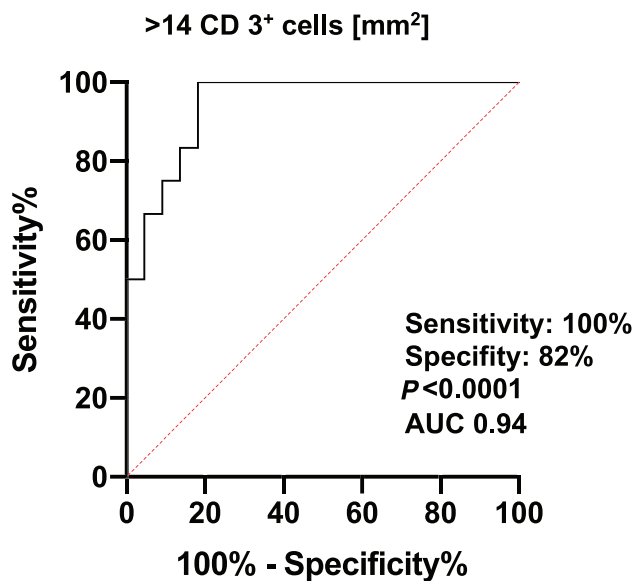
Analysis of myocardial oedema and function

Cardiovascular magnetic resonance measurements in a subset of patients (*n* = 21; 0R = 17; 1R = 4) revealed values in the normal range for LV end diastolic diameter (49.5 ± 5.9 mm), LV end systolic diameter (31.6 ± 5.3 mm), and LV mass (105.4 ± 22.2 g) (*Table 3*).[28] Due to little numbers in the 1R group, no comparing statistics between the groups were performed. Functional measurements of LV ejection fraction using echocardiography in all patients and cardiac index measurements using a modified Fick method revealed comparable values within the normal range for both groups. Groups did not differ in HF symptoms, acquired as NYHA class (*Table 1*).

Table 3 Cardiovascular magnetic resonance

	All patients (n = 21)	Normal values mean ± SD; lower–upper limits28
LVEDD (mm)	49.5 ± 5.9	52 ± 5; 42–62
LVESD (mm)	31.6 ± 5.3	32 ± 3; 26–38
IVS (mm)	12.9 ± 1.8	15 ± 3; 7–23
LVEDV (mL)	114.5 ± 30.3	155 ± 30; 95–215
LVESV (mL)	39.6 ± 15.6	55 ± 15; 25–85
LVSV (mL)	74.9 ± 17.7	103 ± 21; 61–145
LV mass (g)	105.4 ± 22.2	121 ± 28; 66–176
LVEF (%)	66.3 ± 7	64 ± 8; 49–79
CO LV (L/min)	5.8 ± 1.1	5.6 ± 1.1; 3.4–7.8
RVEF (%)	65 ± 7.3	66 ± 7; 51–80
CO RV (L/min)	6 ± 1.2	5.6 ± 1.4; 2.8–8.3

CO, cardiac output; IVS, interventricular septum; LV, left ventricle; LVEDD, left ventricular end diastolic diameter; LVEDV, left ventricular end diastolic volume; LVEF, left ventricular ejection fraction; LVESD, left ventricular end systolic diameter, LVESV, left ventricular end systolic volume; RV, right ventricle.
Means ± SD.

Cardiovascular magnetic resonance analysis revealed an inverse correlation of global LV T2 relaxation time, a marker of myocardial oedema, to myocardial mitochondrial state III respiration supported by octanoyl-L-carnitine for CETF and glutamate for mitochondrial complex I respiration (CETF; *r* = −0.62, *P* = 0.002; CETF + CI *r* = −0.48, *P* = 0.02; *Figure 4*).

Uncoupled mitochondrial respiration correlated with peak systolic global longitudinal strain, indicating progressive systolic dysfunction parallel to declining uncoupled myocardial mitochondrial respiration (*r* = −0.63, *P* = 0.004; *Figure 5*).

Inflammatory cell infiltration relates to impaired myocardial mitochondrial respiration

Immunohistochemical staining and quantitative assessment of CD3$^+$ T lymphocytes infiltrating the myocardium was significantly inversely correlated to myocardial mitochondrial state III supported by the fatty acid octanoyl-L-carnitine (CETF; *r* = −0.41, *P* = 0.02; *Figure 6*). Parallel to these results, mitochondrial complex I respiration supported by octanoyl-L-carnitine and glutamate correlated inversely to myocardial CD3$^+$ T lymphocyte infiltration (CETF + CI *r* = −0.35, *P* = 0.04; *Figure 6*).

Oxidative stress in impaired mitochondrial respiration

Thiobarbituric acid reactive substances measurement as a marker of systemic oxidative stress in serum samples revealed a correlation to lower uncoupled mitochondrial respiration (*r* = −0.42, *P* = 0.001). Likewise, static oxidation–reduction potentials (sORP) correlated inversely to uncoupled mitochondrial respiration (*r* = −0.38, *P* = 0.03; *Figure 5*).

Figure 4 Impaired myocardial mitochondrial respiration relates to global T2 relaxation time in cardiac MRI. Pearson correlation coefficients across both groups with linear regression line. *n* = 23 (18 vs. 5). Substrates used were octanoyl-L-carnitine (for CETF), glutamate (for CI); CETF, electron transferring flavoprotein complex; CI, respiratory chain complex I; MRI, magnetic resonance imaging.
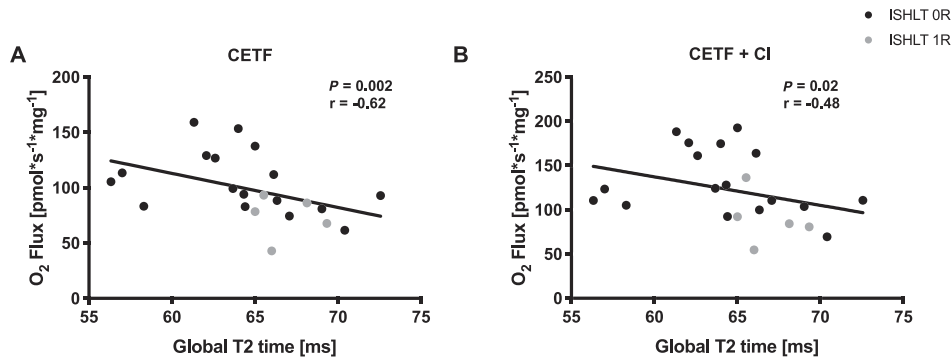
Figure 5 Uncoupled mitochondrial respiration relates to oxidative stress and left ventricular dysfunction. Uncoupled myocardial mitochondrial respiration in endomyocardial biopsies with no ACR (0R) (*n* = 23) or mild ACR (1R) (*n* = 12) cellular heart transplant rejection after stepwise titration of carbonyl cyanide-trifluoromethoxyphenylhydrazone (FCCP) correlates inverse to markers of oxidative stress [(A) Thiobarbituric acid reactive substances (TBARS); (B) static oxidation–reduction potential (sORP); (C) peak systolic global longitudinal strain (GLS) in cardiac magnetic resonance analysis; Spearman correlation.
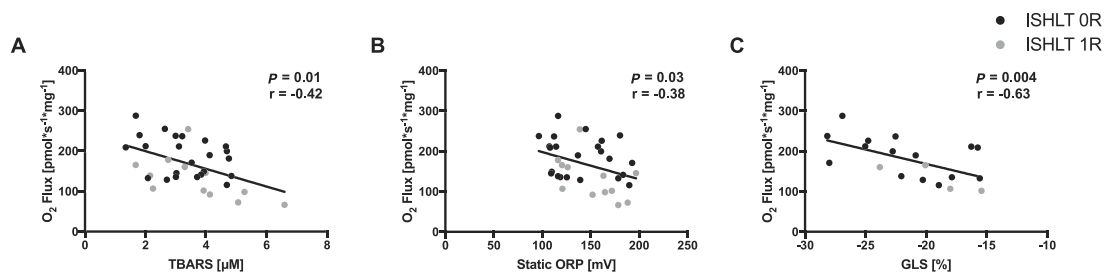
Figure 6 CD 3[+] cell infiltration relates to impaired myocardial mitochondrial respiration. Spearman correlation coefficients across both groups with linear regression line. Myocardial infiltration with CD3^{+} cells relates to an impaired myocardial mitochondrial respiration. *n* = 34 (22 vs. 12). Substrates used were octanoyl-L-carnitine (for CETF) and glutamate (for CI). CETF, electron transferring flavoprotein complex; CI, respiratory chain complex I.
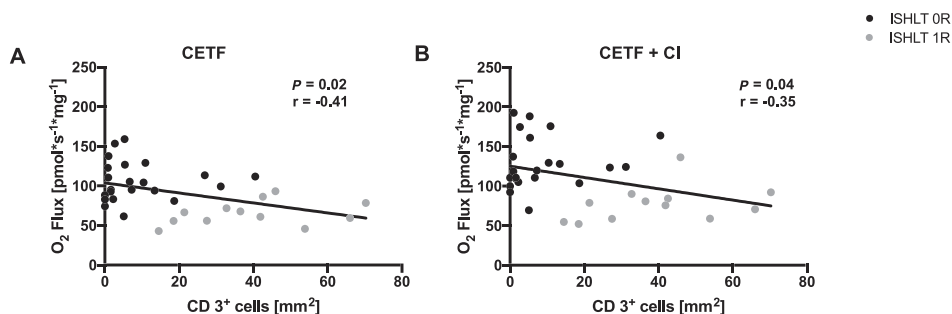
Discussion

In this study, we report disturbed mitochondrial bioenergetics accompanying inflammatory cell infiltration in human heart transplant recipients. The main findings are as follows: (i) cardiac allograft recipients with mild ACR (1R) display lower myocardial mitochondrial respiration compared with ACR (0R), (ii) myocardial inflammation, systemic oxidative stress, and myocardial oedema are related to disturbed mitochondrial respiration and subclinical myocardial dysfunction and (iii) quantitative assessment of infiltrating CD3^{+} T lymphocytes distinguished reliable ACR (1R) from ACR (0R).

Myocardial bioenergetics

Despite the fact of similar clinical features of the patients, mitochondrial respiration was impaired already in ACR (1R) suggesting a rejection related functional impairment in our patients. Disturbed myocardial bioenergetics have been shown to play a pivotal role in HF pathophysiology.[15] Previously, we showed that oxidative capacity in myocardial tissue specimens from terminal HF patients undergoing LVAD surgery or HTX also was about 40% decreased compared with stable heart transplant recipients with a normal LV function without ACR undergoing surveillance EMB.[16] Myocardial mitochondrial respiration correlated with cardiac index measurements.[16] Likewise, other groups described an about 40% diminished OXPHOS capacity in LV tissue specimens on non-fatty acid substrates or octanoylcarnitine in patients undergoing LVAD surgery.[15] Although there are numerous reasons why a human heart can fail, mismatch between ATP supply and demand can at least partly account for worsening of the HF state.[29] Gvozdjakova *et al*. observed an impaired myocardial mitochondrial respiration in ACR.[19] These observations were not linked to clinical or haemodynamic characteristics of the patients, and immunohistochemistry of infiltrating inflammatory cells was not performed.

Here, we observe impairment of mitochondrial respiration in ACR (1R) in a range so far only known from patients with advanced HF. We observed impaired OXPHOS capacity in ACR (1R) compared with ACR (0R) with regard to different substrate combinations (*Figure 1A–D*). Moreover, we detected reduced respiratory control ratio (*Figure 1E*) indicating impaired mitochondrial coupling efficiency in ACR (1R) which is independent of mitochondrial content and suggests a less efficient ATP production.[30–32] Romero *et al*. described a decreased activity of mitochondrial-related genes in ACR.[20] Our results complement these findings and suggest the translation of alterations in mitochondrial gene regulation in functional alterations. These findings expose mitochondrial dysfunction as a potential therapeutic target in ACR, especially considering promising effects of dietary interventions on mitochondrial bioenergetics.[33,34] Just recently, a dipeptidyl peptidase-4 inhibitor and the inhibitor of the sodium-glucose linked transporter 2 ertugliflozin have been shown to improve mitochondrial oxidative phosphorylation, whether these effects can be transferred to mitochondrial dysfunction in ACR is yet unclear.[35,36]

Oxidative stress

Impaired mitochondrial respiration in patients suffering from HF has been associated with excessive mitochondrial ROS release and a reduced ATP production.[37,38] According to these findings in HF patients, we observed an inverse correlation of the systemic oxidative stress markers thiobarbituric acid

reactive substances and oxidation–reduction potentials with mitochondrial respiration (*Figure 5A,B*). ROS accumulation has been described to be a source of mitochondrial genomic instability, leading to mitochondrial DNA damage resulting in altered mitochondrial function.[39] ACR is associated with ROS production, so ROS induced mitochondrial genomic instability may be one potential pathway for ACR mediated mitochondrial dysfunction.[40] Described impairments in mitochondrial bioenergetics are related to higher global T2 times in CMR measurements of our patients (*Figure 4A,B*), indicating myocardial oedema and inflammation, suggesting that the observed bioenergetic changes are already reflected in cardiac functional imaging.[41–43] Leaking sarcoplasmic reticulum calcium channels have been shown to provoke mitochondrial calcium overload and dysfunction in HF, ACR associated dysfunction of sarcoplasmic reticulum may turn out to be yet another driver of mitochondrial dysfunction.[44]

Quantitative immunohistochemistry

Infiltration of CD3+ lymphocytes was associated with impaired mitochondrial respiration (*Figure 4*). Because gold standard analysis of myocardial mitochondrial respiration using high respiration respirometry is complex and time consuming, analysing infiltrating CD3+ lymphocytes may have the potential for estimating mitochondrial respiration and therapy monitoring. The CD3 T cell receptor is involved in both activating CD8+ cytotoxic T cells and CD4+ T helper cells. Because CD 4+ T lymphocytes are the predominantly infiltrating mononuclear cells in ACR, quantitative CD3 T lymphocyte monitoring, as it is established for diagnosis of myocarditis, seems also a reasonable for ACR monitoring.[6]

Even in the absence of ACR according to light microscopy, computer-based quantification of infiltrating inflammatory cells revealed some amount of T lymphocyte infiltration.[4] This observation supports the recently described important role of infiltrating T lymphocytes not only in acute myocarditis and ACR, but also in other pathological states like ischaemia, dilative cardiomyopathy, arterial hypertension, arteriosclerosis, and aging.[45] Analysing inflammatory cell infiltration in EMB of HTX patients with ACR (1R) compared with ACR (0R) revealed a more than four times higher infiltration of CD3+ T lymphocytes in ACR (1R) rejection (*Table 3*).

In HF, it has been shown that T-cell immune response resulted in acute and chronic inflammatory processes impairing cardiac function by direct cytotoxicity or by enhancing the inflammatory functions of other cells. Further studies are needed to investigate a direct effect of infiltrating immune cells on mitochondrial bioenergetics.[45]

In 2004, the ISHLT ACR grading scheme was revised, among others to improve reproducibility. Comparing interobserver reproducibility of the 1990 and 2004 ISHLT ACR grading scheme, only a small, non-significant improvement was

observed.[46] Digital image analysis of infiltrating inflammatory cells has the potential to detect ACR with high reproducibility. In similar way, this has recently been revealed for the diagnostic workup of acute myocarditis,[47] thus current diagnostic criteria for acute myocarditis comprise an absolute quantification of infiltrating inflammatory cells using immunohistochemistry in addition to histological findings.[21] The immunohistochemical value for the diagnosis of myocarditis ($\geq$14 leucocytes/mm^2 including up to 4 monocytes/mm^2 with the presence of CD 3 positive T lymphocytes $\geq$7 cells/mm^2) corresponds well to the results of our ROC analysis where immunohistochemically detection of an endomyocardial infiltration >14 CD3$^+$ cells/mm^2 discriminated the histological diagnosis of ACR (0R) vs. ACR (1R) rejection with a sensitivity of 100% and a specify of 82% (*Figure 3*). Further evaluation of inflammatory cell infiltration in correlation to clinical parameters, outcome analysis and response to treatment is needed to assess the diagnostic power of this approach.

Here, adaptation of immunohistochemical standards for the diagnosis of myocardial inflammation allowed discrimination of mild ACR (1R) from ACR (0R). Ongoing studies validate whether analysis of the CD3$^+$ T lymphocytes also identifies moderate ACR (2R) and severe ACR (3R) rejection and whether an absolute CD3$^+$ cell count has a prognostic impact in heart transplant recipients. If so, analysing myocardial infiltration of CD3$^+$ lymphocytes could be a promising diagnostic tool to tailor immunosuppressive therapy.

Limitations

Some limitations apply to this study. We performed a cross-sectional prospective trial including heart transplant recipients. Due to the single-centre design of the trial, quantity of participants is limited. The amount of human ventricular myocardial tissue harvested in EMB limited the implementable number of experiments. Furthermore, during our inclusion period, only three cases of ACR (2R), and no case of ACR (3R) occurred, which was not sufficient for statistical analyses of these groups in the study. Like other studies analysing human ventricular tissue specimens, mitochondrial respiration in HTX recipients was not compared with tissue specimens of a heathy control group due to the impossibility of receiving heathy tissue specimens. Assessment of long-term data from the presented cohort will address the impact of impaired mitochondrial bioenergetics and inflammatory cell infiltration on cardiac function, clinical symptoms, and endpoints (death and rehospitalization).

Conclusions

Mild ACR with inflammatory cell infiltration associates with impaired mitochondrial bioenergetics in cardiomyocytes. Digital image analysis with quantification of infiltrating inflammatory cells identifies patients with mild ACR reliable. Our findings may help to identify novel checkpoints in cardiac immune metabolism as potential therapeutic targets in post-transplant care.

Acknowledgements

Conflict of interest

None of the authors has a financial relationship with a commercial entity that has an interest in the subject of the presented manuscript or other conflicts of interest to disclose.

Funding

Author contributions

Data acquisition, experimental procedures, organization, writing of the first draft, discussion, and writing of the final draft were performed by D.S.; data acquisition, experimental procedures, and discussion by E.Z., S.A., and M.S.; organization, conception, discussion, and writing of the final draft by T.J.; data acquisition, discussion, writing of the final draft by P.H. and F.B.; data acquisition, organization, discussion, and writing of the final draft by H.P.S., G.A., and F.E.; data acquisition, organization, and discussion by U.B. and P.A.; organization, discussion, and writing of the final draft by M.K. and M.R.; initial conception, data acquisition, organization, discussion, and writing of the final draft by J.S. and R.W.

Data availability statement

The datasets generated during and/or analysed during the current study are available from the corresponding author on reasonable request.

References

1. Ponikowski P, Voors AA, Anker SD, Bueno H, Cleland JGF, Coats AJS, Falk V, González-Juanatey JR, Harjola VP, Jankowska EA, Jessup M, Linde C, Nihoyannopoulos P, Parissis JT, Pieske B, Riley JP, Rosano GMC, Ruilope LM, Ruschitzka F, Rutten FH, van der Meer P, Authors/Task Force Members, Document Reviewers. 2016 ESC guidelines for the diagnosis and treatment of acute and chronic heart failure: the task force for the diagnosis and treatment of acute and chronic heart failure of the European Society of Cardiology (ESC). Developed with the special contribution of the Heart Failure Association (HFA) of the ESC. *Eur J Heart Fail* 2016; **18**: 891–975.

2. Khush KK, Cherikh WS, Chambers DC, Harhay MO, Hayes D Jr, Hsich E, Meiser B, Potena L, Robinson A, Rossano JW, Sadavarte A, Singh TP, Zuckermann A, Stehlik J, International Society for Heart and Lung Transplantation. The International Thoracic Organ Transplant Registry of the International Society for Heart and Lung Transplantation: thirty-sixth adult heart transplantation report-2019; focus theme: donor and recipient size match. *J Heart Lung Transplant* 2019; **38**: 1056–1066.

3. Gradek WQ, D'Amico C, Smith AL, Vega D, Book WM. Routine surveillance endomyocardial biopsy continues to detect significant rejection late after heart transplantation. *J Heart Lung Transplant* 2001; **20**: 497–502.

4. Stewart S, Winters GL, Fishbein MC, Tazelaar HD, Kobashigawa J, Abrams J, Andersen CB, Angelini A, Berry GJ, Burke MM, Demetris AJ, Hammond E, Itescu S, Marboe CC, McManus B, Reed EF, Reinsmoen NL, Rodriguez ER, Rose AG, Rose M, Suciu-Focia N, Zeevi A, Billingham ME. Revision of the 1990 working formulation for the standardization of nomenclature in the diagnosis of heart rejection. *J Heart Lung Transplant* 2005; **24**: 1710–1720.

5. Taylor DO, Edwards LB, Aurora P, Christie JD, Dobbels F, Kirk R, Rahmel AO, Kucheryavaya AY, Hertz MI. Registry of the International Society for Heart and Lung Transplantation: twenty-fifth official adult heart transplant report—2008. *J Heart Lung Transplant* 2008; **27**: 943–956.

6. Higuchi MD, Gutierrez PS, Aiello VD, Palomino S, Bocchi E, Kalil J, Bellotti G, Pileggi F. Immunohistochemical characterization of infiltrating cells in human chronic chagasic myocarditis—comparison with myocardial rejection process. *Virchows Arch A* 1993; **423**: 157–160.

7. Costanzo MR, Dipchand A, Starling R, Anderson A, Chan M, Desai S, Fedson S, Fisher P, Gonzales-Stawinski G, Martinelli L, McGiffin D. The International Society of Heart and Lung Transplantation Guidelines for the care of heart transplant recipients. *J Heart Lung Transplant* 2010; **29**: 914–956.

8. Brunner-La Rocca HP, Sutsch G, Schneider J, Follath F, Kiowski W. Natural course of moderate cardiac allograft rejection (International Society for Heart Transplantation grade 2) early and late after transplantation. *Circulation* 1996; **94**: 1334–1338.

9. Stride N, Larsen S, Hey-Mogensen M, Hansen CN, Prats C, Steinbrüchel D, Køber L, Dela F. Impaired mitochondrial function in chronically ischemic human heart. *Am J Physiol Heart Circ Physiol* 2013; **304**: H1407–H1414.

10. Stanley WC, Chandler MP. Energy metabolism in the normal and failing heart: Potential for therapeutic interventions. *Heart Fail Rev* 2002; **7**: 115–130.

11. Taegtmeyer H. Cardiac metabolism as a target for the treatment of heart failure. *Circulation* 2004; **110**: 894–896.

12. Quiroga C, Mancilla G, Oyarzun I, Tapia A, Caballero M, Gabrielli LA, Valladares-Ide D, Del Campo A, Castro PF, Verdejo HE. Moderate exercise in spontaneously hypertensive rats is unable to activate the expression of genes linked to mitochondrial dynamics and biogenesis in cardiomyocytes. *Front Endocrinol (Lausanne)* 2020; **11**: 546.

13. Chaanine AH, LeJemtel TH, Delafontaine P. Mitochondrial pathobiology and metabolic remodeling in progression to overt systolic heart failure. *J Clin Med* 2020; **9**.

14. Gambardella J, Sorriento D, Ciccarelli M, del Giudice C, Fiordelisi A, Napolitano L, Trimarco B, Iaccarino G, Santulli G. Functional role of mitochondria in arrhythmogenesis. *Adv Exp Med Biol* 2017; **982**: 191–202.

15. Stride N, Larsen S, Hey-Mogensen M, Sander K, Lund JT, Gustafsson F, Køber L, Dela F. Decreased mitochondrial oxidative phosphorylation capacity in the human heart with left ventricular systolic dysfunction. *Eur J Heart Fail* 2013; **15**: 150–157.

16. Scheiber D, Jelenik T, Zweck E, Horn P, Schultheiss HP, Lassner D, Boeken U, Saeed D, Kelm M, Roden M, Westenfeld R. High-resolution respirometry in human endomyocardial biopsies shows reduced ventricular oxidative capacity related to heart failure. *Exp Mol Med* 2019; **51**: 1–10.

17. Duboc D, Abastado P, Muffat-Joly M, Perrier P, Toussaint M, Marsac C, Francois D, Lavergne T, Pocidalo JJ, Guerin F. Evidence of mitochondrial impairment during cardiac allograft rejection. *Transplantation* 1990; **50**: 751–755.

18. Abastado P, Duboc D, Marsac C, Muffat-Joly M, Toussaint M, Perier P, François D, Carpentier A, Valty J, Guérin F. Demonstration of abnormalities of myocardial mitochondrial oxygenation in cardiac graft rejection. *Arch Mal Coeur Vaiss* 1991; **84**: 855–859 Mise en evidence d'anomalies de l'oxydation mitochondriale myocardique au cours du rejet de greffe cardiaque.

19. Gvozdjakova A, Kucharska J, Mizera S, Braunová Z, Schreinerová Z, Schrameková E, Pecháň I, Fabián J. Coenzyme Q10 depletion and mitochondrial energy disturbances in rejection development in patients after heart transplantation. *Biofactors* 1999; **9**: 301–306.

20. Romero E, Chang E, Tabak E, Pinheiro D, Tallaj J, Litovsky S, Keating B, Deng M, Cadeiras M. Rejection-associated mitochondrial impairment after heart transplantation. *Transplant Direct* 2020; **6**: e616.

21. Caforio AL, Pankuweit S, Arbustini E, Basso C, Gimeno-Blanes J, Felix SB, Fu M, Heliö T, Heymans S, Jahns R, Klingel K. Current state of knowledge on aetiology, diagnosis, management, and therapy of myocarditis: A position statement of the European Society of Cardiology Working Group on myocardial and pericardial diseases. *Eur Heart J* 2013; **34**: 2636–2648.

22. Scheiber D, Zweck E, Jelenik T, Horn P, Albermann S, Masyuk M, Boeken U, Saeed D, Kelm M, Roden M, Szendroedi J, Westenfeld R. Reduced myocardial mitochondrial ROS production in mechanically unloaded hearts. *J Cardiovasc Transl Res* 2019; **12**: 107–115.

23. Jelenik T, Flogel U, Alvarez-Hernandez E, Scheiber D, Zweck E, Ding Z, Rothe M, Mastrototaro L, Kohlhaas V, Kotzka J, Knebel B. Insulin resistance and vulnerability to cardiac ischemia. *Diabetes* 2018; **67**: 2695–2702.

24. Spieker M, Haberkorn S, Gastl M, Behm P, Katsianos S, Horn P, Jacoby C, Schnackenburg B, Reinecke P, Kelm M, Westenfeld R. Abnormal T2 mapping cardiovascular magnetic resonance correlates with adverse clinical outcome in patients with suspected acute myocarditis. *J Cardiovasc Magn Reson* 2017; **19**: 1–9.

25. Osinska I, Popko K, Demkow U. Perforin: an important player in immune response. *Cent Eur J Immunol* 2014; **39**: 109–115.

26. Escher F, Kuhl U, Lassner D, Stroux A, Westermann D, Skurk C, Tschöpe C, Poller W, Schultheiss HP. Presence of perforin in endomyocardial biopsies of patients with inflammatory cardiomyopathy predicts poor outcome. *Eur J Heart Fail* 2014; **16**: 1066–1072.

27. Miyawaki T, Kasahara Y, Kanegane H, Ohta K, Yokoi T, Yachie A, Taniguchi N. Expression of Cd45r0 (Uchl1) by Cd4+ and Cd8+ T-cells as a sign of in vivo

activation in infectious-mononucleosis. *Clin Exp Immunol* 1991; **83**: 447–451.

28. Kawel-Boehm N, Hetzel SJ, Ambale-Venkatesh B, Captur G, Francois CJ, Jerosch-Herold M, Salerno M, Teague SD, Valsangiacomo-Buechel E, Van der Geest RJ, Bluemke DA. Reference ranges ("normal values") for cardiovascular magnetic resonance (CMR) in adults and children: 2020 update. *J Cardiovasc Magn Reson* 2020; **22**: 87.

29. Neubauer S. The failing heart—an engine out of fuel. *N Engl J Med* 2007; **356**: 1140–1151.

30. Pesta D, Gnaiger E. High-resolution respirometry: OXPHOS protocols for human cells and permeabilized fibers from small biopsies of human muscle. *Methods Mol Biol* 2012; **810**: 25–58.

31. Koliaki C, Szendroedi J, Kaul K, Jelenik T, Nowotny P, Jankowiak F, Herder C, Carstensen M, Krausch M, Knoefel WT, Schlensak M. Adaptation of hepatic mitochondrial function in humans with non-alcoholic fatty liver is lost in steatohepatitis. *Cell Metab* 2015; **21**: 739–746.

32. Gnaiger E. Capacity of oxidative phosphorylation in human skeletal muscle: new perspectives of mitochondrial physiology. *Int J Biochem Cell Biol* 2009; **41**: 1837–1845.

33. Xiang C, Zhang F, Gao J, Guo F, Zhang M, Zhou R, Wei J, Wang P, Zhang Y, Zhang J, Yang H. Yixin-Shu capsules ameliorated ischemia-induced heart failure by restoring Trx2 and inhibiting JNK/p38 activation. *Oxid Med Cell Longev* 2021; **2021**: 8049079.

34. Rennison JH, McElfresh TA, Okere IC, Patel HV, Foster AB, Patel KK, Stoll MS, Minkler PE, Fujioka H, Hoit BD, Young ME. Enhanced acyl-CoA dehydrogenase activity is associated with improved mitochondrial and contractile function in heart failure. *Cardiovasc Res* 2008; **79**: 331–340.

35. Takada S, Masaki Y, Kinugawa S, Matsumoto J, Furihata T, Mizushima W, Kadoguchi T, Fukushima A, Homma T, Takahashi M, Harashima S, Matsushima S, Yokota T, Tanaka S, Okita K, Tsutsui H. Dipeptidyl peptidase-4 inhibitor improved exercise capacity and mitochondrial biogenesis in mice with heart failure via activation of glucagon-like peptide-1 receptor signalling. *Cardiovasc Res* 2016; **111**: 338–347.

36. Croteau D, Luptak I, Chambers JM, Hobai I, Panagia M, Pimentel DR, Siwik DA, Qin F, Colucci WS. Effects of sodium-glucose linked transporter 2 inhibition with ertugliflozin on mitochondrial function, energetics, and metabolic gene expression in the presence and absence of diabetes mellitus in mice. *J Am Heart Assoc* 2021; **10**: e019995.

37. Sharov VG, Todor AV, Silverman N, Goldstein S, Sabbah HN. Abnormal mitochondrial respiration in failed human myocardium. *J Mol Cell Cardiol* 2000; **32**: 2361–2367.

38. Song MS, Chen Y, Gong GH, Murphy E, Rabinovitch PS, Dorn GW. Super-suppression of mitochondrial reactive oxygen species signaling impairs compensatory autophagy in primary mitophagic cardiomyopathy. *Circ Res* 2014; **115**: 348–353.

39. Ayoub KF, Pothineni NVK, Rutland J, Ding Z, Mehta JL. Immunity, inflammation, and oxidative stress in heart failure: emerging molecular targets. *Cardiovasc Drugs Ther* 2017; **31**: 593–608.

40. Pieper GM, Nilakantan V, Nguyen TK, Hilton G, Roza AM, Johnson CP. Reactive oxygen and reactive nitrogen as signaling molecules for caspase 3 activation in acute cardiac transplant rejection. *Antioxid Redox Signal* 2008; **10**: 1031–1040.

41. Lota AS, Gatehouse PD, Mohiaddin RH. T2 mapping and T2* imaging in heart failure. *Heart Fail Rev* 2017; **22**: 431–440.

42. Greulich S, Ferreira VM, Dall'Armellina E, Mahrholdt H. Myocardial inflammation—are we there yet? *Curr Cardiovasc Imaging Rep* 2015; **8**: 6.

43. Giri S, Chung YC, Merchant A, Mihai G, Rajagopalan S, Raman SV, Simonetti OP. T2 quantification for improved detection of myocardial edema. *J Cardiovasc Magn Reson* 2009; **11**: 56.

44. Santulli G, Xie W, Reiken SR, Marks AR. Mitochondrial calcium overload is a key determinant in heart failure. *Proc Natl Acad Sci U S A* 2015; **112**: 11389–11394.

45. Blanton RM, Carrillo-Salinas FJ, Alcaide P. T-cell recruitment to the heart: friendly guests or unwelcome visitors? *Am J Physiol Heart Circ Physiol* 2019; **317**: H124–H140.

46. Yang HM, Lai CK, Gjertson DW, Baruch-Oren T, Ra SH, Watts W, Wallace WD, Shintaku P, Kobashigawa JA, Fishbein MC. Has the 2004 revision of the International Society of Heart and Lung Transplantation grading system improved the reproducibility of the diagnosis and grading of cardiac transplant rejection? *Cardiovasc Pathol* 2009; **18**: 198–204.

47. Basso C, Calabrese F, Angelini A, Carturan E, Thiene G. Classification and histological, immunohistochemical, and molecular diagnosis of inflammatory myocardial disease. *Heart Fail Rev* 2013; **18**: 673–681.